

Microstructure and magnetic properties of tubular cobalt–silica nanocomposites

Lirong Ren^{a,c}, Lin He^b, Chinping Chen^b, Michael Wark^c, Chunping Li^a,
Ping Che^a, Lin Guo^{a,*}

^a*School of Materials Science and Engineering, Beijing University of Aeronautics and Astronautics, Beijing 100083, PR China*

^b*Department of Physics, Peking University, Beijing, 100871, PR China*

^c*Institute for Physical Chemistry and Electrochemistry, University of Hanover, Callinstr. 3-3A, Hannover 30167, Germany*

Received 12 July 2006; received in revised form 28 October 2006

Available online 30 November 2006

Abstract

Co-based (Co and Co₃O₄) nanoparticles were self-integrated into SiO₂ nanotubes with a methodology based on the use of a Co salt as a template structure for the formation of SiO₂ nanotubes. Within the confinement of tubular matrix of SiO₂, the nanofibres of cobalt precursor, i.e., [Co(NH₃)₆](HCO₃)(CO₃)·2H₂O, were treated in a H₂ atmosphere with different parameters. With a sufficient reduction on the cobalt precursor, sphere-like Co-based nanoparticles are obtained, being well aligned in the interior space of the SiO₂ nanotubes. With an insufficient reduction, platelet-like Co-based nanoparticles are formed, being arranged in a random manner inside the SiO₂ nanotubes. The sufficiently reduced Co–SiO₂ nanocomposite exhibits an open hysteresis loop in the low field region (<3 kOe) and a paramagnetic response in high field (>3 kOe) at 300 K. An observed wide separation between the zero-field-cooling (ZFC) and field-cooling (FC) curves over the whole temperature region has demonstrated a characteristic feature of ferromagnetism with a magnetically anisotropic barrier diverting the easy axis from the axis of the applied field. The predominant factor leading to this anisotropic potential barrier is attributed to the shape anisotropy native to the one-dimensional arrangement of Co-based nanoparticles within the tubular matrix, i.e. SiO₂ nanotubes.

© 2006 Elsevier B.V. All rights reserved.

Keywords: Magnetic properties; Silica nanotubes; Cobalt; Nanocomposite

1. Introduction

The dispersion and stabilization of freshly prepared magnetic nanoparticles have become hot topics for different systems and composites. Magnetic particles in ferrofluids [1,2] are protected from oxidation and agglomeration by surfactant molecules covering the particle surfaces. In Co–Au [3], CoFe–Au/Ag [4] or oxide-passivated Co [5], Fe [6,7], CoFe [5,8] particles, the core–shell morphology can effectively stabilize the dispersive system. In nanocomposites such as Co–Al₂O₃ [9], Fe–Al₂O₃ [10,11] magnetic particles are embedded in a chemically dissimilar matrix. The influences of the dispersants, i.e., surfactants, shells or matrices, on the

magnetic properties of the dispersive systems have been extensively studied.

Co–SiO₂ nanocomposites with porous SiO₂ as matrix are not yet fully studied magnetically [12]. They are particularly attractive as supported Co catalysts for Fischer–Tropsch synthesis, i.e. the conversion of synthetic gas to long-chain hydrocarbons [13–15]. The conventional preparation of Co–SiO₂ nanocomposites is mainly based on aqueous impregnation of the porous oxide with solutions of Co salts. The SiO₂-supported catalysts are prepared after the decomposition of the supported Co salt via calcination in air and subsequent reduction process in an atmosphere of H₂ [13]. Recently, a novel Co–SiO₂ nanocomposite consisting of aligned sphere-like nanoparticles of Co within SiO₂ nanotubes was developed by employing accurately tailored nanofibres of a Co salt as templates in a sol–gel process [16]. The calcination in H₂

*Corresponding author. Tel./fax: +86 10 82338162.

E-mail address: guolin@buaa.edu.cn (L. Guo).

leads to the formation of almost spherical Co nanoparticles, which are well aligned in rows due to magnetic dipolar interactions between neighboring particles in combination with the tube confinement. It is of great interest to investigate the magnetic properties of such tubular Co–SiO₂ nanocomposite for both fundamental and practical purposes.

In this paper, detailed magnetic data on this novel Co–SiO₂ nanocomposite are reported. Samples of the tubular nanocomposites were prepared using different H₂ treatment and studied regarding their microstructures. The influence of the dispersive system, i.e. the tubular matrix of SiO₂, on the temperature dependency of magnetization of the tubular Co–SiO₂ nanocomposite is discussed.

2. Experimental

The detailed preparation of tubular Co–SiO₂ nanocomposite has been described previously [16]. In brief, nanofibers of [Co(NH₃)₆](HCO₃)(CO₃)·2H₂O were precipitated from its aqueous solution by solvent modification and then used as templates for the formation of SiO₂ walls in a sol–gel process. The as-prepared SiO₂ nanotubes were subjected to H₂ (6 L/h) reduction with a heating rate of 5 °C/min at 400 °C for 4 h (sample S1) or at 300 °C for 1 h (sample S2). The structure and composition of both samples were characterized by transmission electron microscopy (TEM) and selected area diffraction pattern (SAED) mainly on a JEOL 2100F microscope. The collective magnetic characterizations were performed on a Quantum Design superconducting quantum interference device (SQUID) magnetometer (MPMS-XL).

3. Results and discussions

The bright-field TEM image in Fig. 1a shows that the sample S1 comprises SiO₂ nanotubes (100–220 nm in diameter) encapsulating a row of well-aligned, sphere-like particles (ca. 10–70 nm). There is a distribution of rows with different widths inside SiO₂ nanotubes. The row width may be related to the width of the templates, i.e. nanofibers of Co precursor inside the tubes. Noteworthy, from the TEM image of a bundle of tubes in Fig. 1b, neighboring nanoparticles seem to be fused together to form short nanowires (indicated with a white arrow). The particles are polycrystalline on the basis of the SAED pattern exhibited in Fig. 1c, being a mixture of hexagonal Co (JPCD5-727) and cubic Co₃O₄ (JPCD80-1535). The ratio of metallic Co inside S1, however, is difficult to be quantified by techniques like X-ray photoelectron spectroscopy due to the tube walls that is about 50-nm thick. The alignment of Co-based particles occurs due to the tube confinement in combination with the magnetic dipolar interactions between neighboring Co particles. SiO₂ nanospheres, one of which is indicated with a black arrow in Fig. 1b, are occasionally present on the external surface of nanotubes.

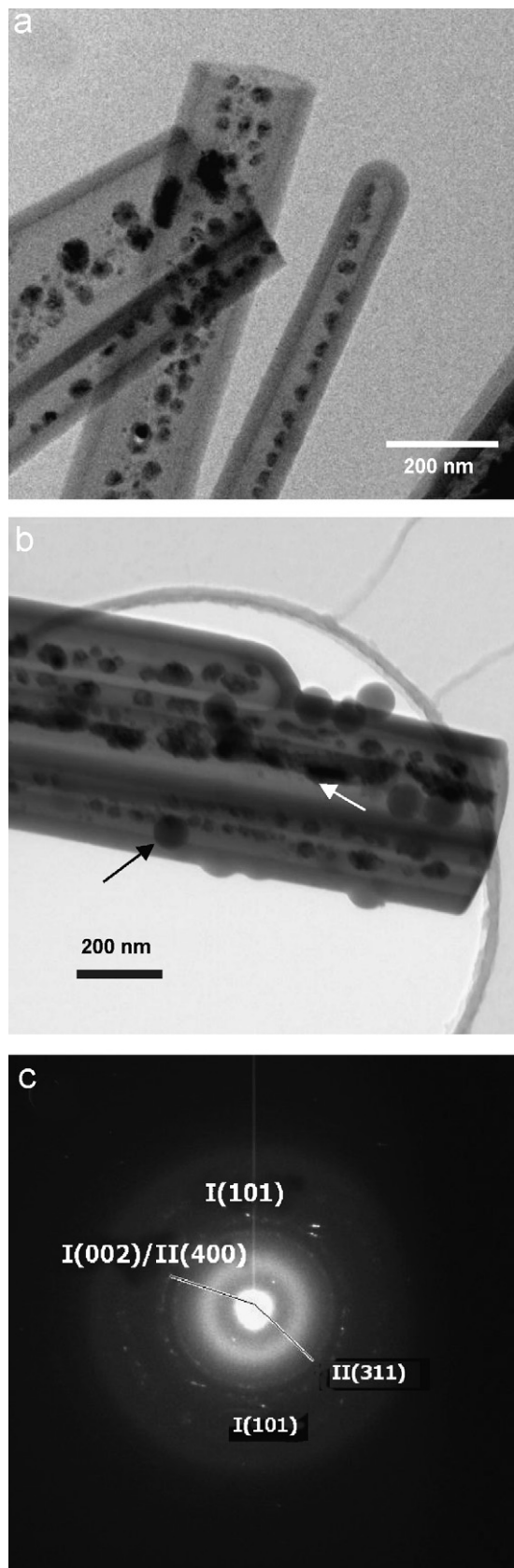


Fig. 1. (a, b) TEM Images of the sufficiently reduced sample S1 and (c) a selected area electron diffraction (SAED) pattern made on the site in Fig. 1b. Diffraction circles and points on the SAED pattern can be assigned to Co (I) and Co₃O₄ (II).

They are the by-products following the rule developed by Stöber et al. [17].

In the insufficiently reduced sample **S2**, tube fillings mostly appear as platelets arranged in a random manner through tube cavities (Fig. 2a). In few cases, (Fig. 2b) both sphere-like and platelet-like particles are present. The fact tells us that the platelet-like Co particles should be precursor structures for the sphere-like nanoparticles. Upon further calcination in a prolonged period and/or at a higher temperature, the unstable platelets curl up and fuse to sphere-like particles. Weak circles of electron diffraction in Fig. 2c could be vaguely assigned to cubic Co_3O_4 (JPCD80-1535). Due to the short treatment of **S2** in H_2 , the level of crystallization of Co_3O_4 in this sample is very limited.

Fig. 3 shows the field and temperature dependence of magnetization for **S1**. The temperature dependence of magnetization has been studied by zero-field-cooling and field-cooling (ZFC/FC) curves between 5 and 395 K. To obtain ZFC curve, the procedure is to cool the sample under zero applied field to 5 K, and then apply a small field of 90 Oe. The magnetization of the sample is recorded in the warming process. For the FC curve the procedure is the same, except that the sample is cooled with the presence of an applied magnetic field of 20 kOe.

In Fig. 3, the FC and ZFC curves separate from each other with the temperature going up to 395 K. This separation should be accounted for by the existence of ferromagnetism with a magnetically anisotropic barrier diverting the easy axis from the axis of the applied field. For the FC measurement, the magnetic moment of each particle is aligned along the orientation of the applied field of 20 kOe with the descending temperature and thereafter frozen at low temperature. After the cooling field is removed, the magnetization, M_{FC} , decreases as the temperature ramps up. This is attributed to the thermal activation effect reorienting the magnetic moment to the orientation of the easy axis, which is along the orientation of magnetic potential minimum. In this case, it is the axis of the nanotube. On the other hand, with the ZFC, the magnetic moments tend to be frozen in randomly distributed orientations when the temperature drops to the low-temperature limit of measurement. With increasing temperature, M_{ZFC} increases due to thermal activation of the magnetic moment. As a consequence, the magnetic moments of the Co nanoparticles align more or less along the field direction. The insets of Fig. 3a show the M - H data for **S1** measured at 300 K. In the low-field region (< 3 kOe), shown in the inset on the right, an open hysteresis loop is apparent with a coercivity of 520 Oe, whereas in the high-field region (> 3 kOe), shown in the inset on the left, a non-saturated linear component reveals the existence of paramagnetism. This notably large coercivity occurs due to the single-domain state of Co particles (10–70 nm) subject to the inter-particle, one-dimensional anisotropic dipolar interaction in the nanotube [16]. The saturated magnetization (M_{S}) of **S1** is determined by extrapolation of

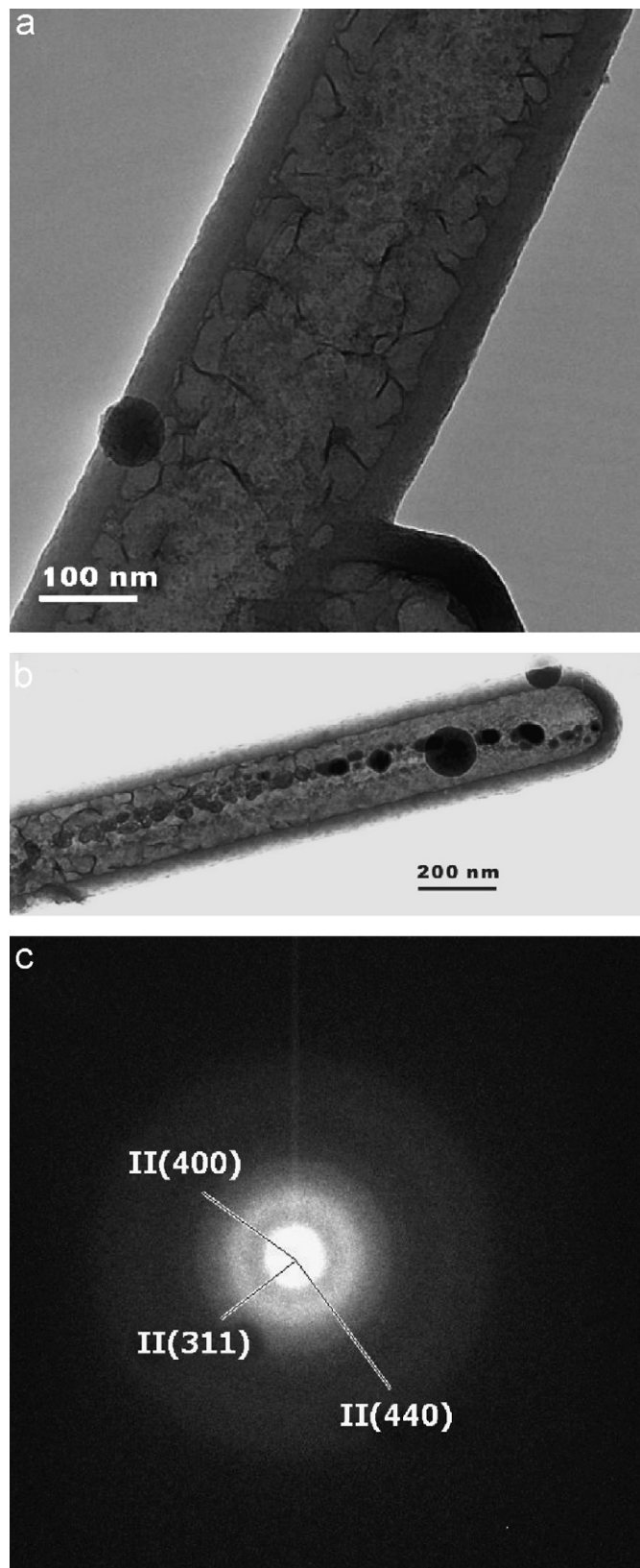


Fig. 2. (a, b) TEM Images of the insufficiently reduced sample **S1** and (c) a selected area electron diffraction (SAED) pattern made on the site in Fig. 2a. The weak circles on SAED can be vaguely assigned to Co_3O_4 (II).

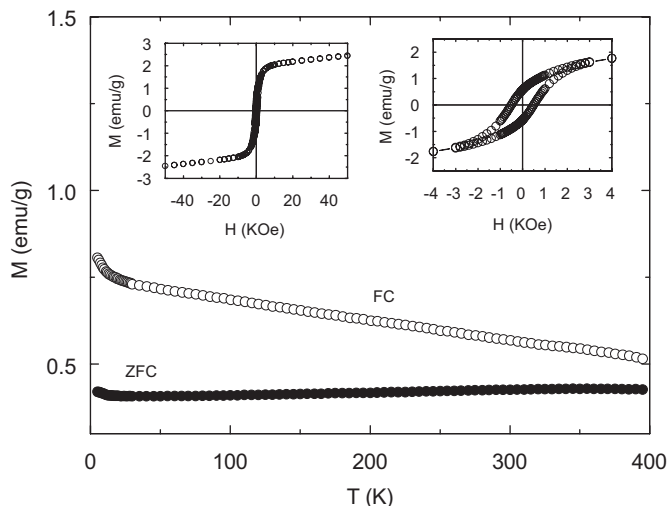


Fig. 3. Magnetic properties of the sufficiently reduced sample S1. The FC and ZFC curves are recorded in a field of 90 Oe with ascending temperature. For the FC, the applied field in the cooling mode is 20 kOe. The insets show the hystereses taken at 300 K.

M versus H to $H = 0$, i.e., ca. 2.0 emu/g (see inset in Fig. 3a). Accordingly, M_S of Co in the tubular Co–SiO₂ nanocomposite (molar ratio of 1:10) can be calculated as 22.3 emu/g_{Co}, or 0.24 μ_B per Co atom, which is roughly 14% of the bulk value. The small M_S value may be attributed to the small-sized particles exhibiting the paramagnetism or superparamagnetism, as is obviously revealed in the high-field region of the hysteresis loop shown in the left inset of Fig. 3a. The remnant magnetization (M_r) is approximately 6.36 emu/g_{Co} and the M_r/M_S ratio is roughly 0.29.

During the thermal treatment in the presence of H₂, the Co precursor, [Co(NH₃)₆](HCO₃)(CO₃)·2H₂O, easily decomposes, leading to the formation of Co₃O₄. In the sufficient reduction process, it is supposed that the initially formed Co₃O₄ would be totally reduced to metallic Co. However, fresh nanoparticles of Co would be unstable upon exposure to air and a layer of Co₃O₄ could form around Co particles, hindering further oxidation. Due to the limited level of crystallization, the existence of Co₃O₄ was not detected by X-ray diffraction in the previous paper [16]. The cubic Co₃O₄ possesses a very similar diffraction pattern as orthorhombic Co₂SiO₄ (JPCD29-0507). The presence of Co₂SiO₄ in the sample, however, can be ruled out because it is much easier to reduce Co₃O₄ to metallic Co than to reduce Co₂SiO₄ [13]. Also the endothermic peaks observed in thermogravimetric analysis of the Co precursor [18] support this assertion, since it is reported that the endothermic decomposition of Co(NO₃)₂ leads to a reducible Co₃O₄, while the high exothermicity of Co(CH₃COO)₂ induces the solid state reaction between SiO₂ and Co oxide and produces a barely reducible Co₂SiO₄ [13]. According to the magnetic study, the antiferromagnetic behavior inherent to Co₃O₄ [19,20] was disguised by the strong ferromagnetic signal of metallic Co.

4. Conclusions

Within the confinement of the tubular matrix of SiO₂, different Co-based (Co and Co₃O₄) nanostructures were formed by different H₂ treatments, including well-aligned, sphere-like nanoparticles after a sufficient H₂ treatment at 400 °C for 4 h (S1) and randomly dispersed platelet-like nanoparticles after an insufficient H₂ treatment at 300 °C for 1 h (S2). A strong ferromagnetic behavior is exhibited in the sufficiently reduced sample S1. The wide separation between the ZFC and FC curves over the whole temperature region demonstrates a characteristic feature of ferromagnetism with a magnetically anisotropic barrier diverting the easy axis, which is the axis of the nanotube, from the axis of the applied field. The interparticle dipolar interaction native to the one-dimensional arrangement of Co-based nanoparticles within the tubular matrix is the predominant factor leading to this anisotropic potential barrier.

Acknowledgments

The authors thank Dr. Armin Feldhoff, Dr. Frank Krumeich, Dr. Xiangcheng Sun, Dr. Xuedong Bai, Dr. Shishen Yan, Dr. Huayong Pan and Dr. Yong Wang for their invaluable help to this work. Support from the National Natural Science Foundation of China (Grant no. 20673009), the Program for New Century Excellent Talents in Universities (NCET-04-0164), Specialized Research Fund for the Doctoral Program of Higher Education (SRFDP-2006006005) as well as Engineering Research Institute, Peking University (ERIPKU-204030) and Deutsche Forschungsgemeinschaft (DFG, WA 1116/8) is gratefully acknowledged.

References

- [1] I. Hrianca, C. Caizer, Z. Schlett, J. Appl. Phys. 92 (2002) 2125.
- [2] A.B. Pakhomov, Y.P. Bao, K.M. Krishnan, J. Appl. Phys. 97 (2005) 10Q305.
- [3] Y. Bao, A.B. Pakhomov, K.M. Krishnan, J. Appl. Phys. 97 (2005) 10J317.
- [4] J.M. Bai, J.P. Wang, Appl. Phys. Lett. 87 (2005) 152502.
- [5] F.J. Darnell, J. Appl. Phys. 32 (1961) 186S.
- [6] L.T. Kuhn, A. Bojesen, L. Timmermann, K. Fauth, E. Coering, E. Johnson, M. Meedom Nielsen, S. Morup, J. Magn. Mater. 272–276 (2004) 1485–1486.
- [7] S. Yu, G.M. Chow, J. Appl. Phys. 98 (2005) 114306.
- [8] Y.W. Zhao, T. Zhang, J.Q. Xiao, J. Appl. Phys. 93 (2003) 8014.
- [9] G.A. Nicklasson, C.G. Granquist, J. Appl. Phys. 55 (1984) 3382.
- [10] J.L. Dormann, C. Djega-Mariadassou, J. Jove, J. Magn. Mater. 104 (1992) 1567.
- [11] C. Djega-Mariadassou, J.L. Dormann, M. Nogues, G. Villers, S. Sayouri, IEEE Trans. Magn. 26 (1990) 1819.
- [12] S.R. Mishra, I. Dubenko, J. Losby, K. Marasinghe, M. Ali, N. Ali, J. Nanosci. Nanotechnol. 5 (2005) 2082.
- [13] J.S. Girardon, A.S. Lermontov, L. Gengembre, P.A. Chernavskii, A. Griboval-Constant, A.Y. Khodakov, J. Catal. 230 (2005) 339.
- [14] P. Dutta, N.O. Elbashir, A. Manivannan, M.S. Seehra, C.B. Roberts, Catal. Lett. 98 (2004) 203.

- [15] Y. Wang, M. Noguchi, Y. Takahashi, Y. Ohtsuka, *Catal. Today* 68 (2001) 3.
- [16] L.R. Ren, L. Guo, M. Wark, Y. Hou, *Appl. Phys. Lett.* 87 (2005) 212503.
- [17] W. Stöber, A. Fink, E. Bohn, *J. Colloid Interface Sci.* 26 (1968) 62.
- [18] L.R. Ren, Ph.D. Thesis, 2004, University of Hanover, Germany.
- [19] R.M. Wang, C.M. Liu, H.Z. Zhang, C.P. Chen, L. Guo, H.B. Xu, S.H. Yang, *Appl. Phys. Lett.* 85 (2004) 2080.
- [20] S.A. Makhlof, *J. Magn. Magn. Mater.* 246 (2002) 184.